DEPARTMENT OF ELECTRICAL AND COMPUTER ENGINEERING
COLLEGE OF ENGINEERING AND TECHNOLOGY
OLD DOMINION UNIVERSITY
NORFOLK, VIRGINIA 23529

AIRBORNE RADAR TECHNOLOGY FOR WINDSHEAR DETECTION

By

Joseph L. Hibey, Principal Investigator

and

Camille S. Khalaf, Graduate Research Assistant

Final Report
For the period ending August 31, 1988

Prepared for the
National Aeronautics and Space Administration
Langley Research Center
Hampton, Virginia 23665

Under
NASA Research Grant NAG-1-626
Dr. Leo D. Staton, Technical Monitor
GCD-Antenna & Microwave Research Branch

July 1988

DEPARTMENT OF ELECTRICAL AND COMPUTER ENGINEERING
COLLEGE OF ENGINEERING AND TECHNOLOGY
OLD DOMINION UNIVERSITY
NORFOLK, VIRGINIA 23529

AIRBORNE RADAR TECHNOLOGY FOR WINDSHEAR DETECTION

By

Joseph L. Hibey, Principal Investigator

and

Camille S. Khalaf, Graduate Research Assistant

Final Report
For the period ending August 31, 1988

Prepared for the
National Aeronautics and Space Administration
Langley Research Center
Hampton, Virginia 23665

Under
NASA Research Grant NAG-1-626
Dr. Leo D. Staton, Technical Monitor
GCD-Antenna & Microwave Research Branch

Submitted by the
Old Dominion University Research Foundation
P. O. Box 6369
Norfolk, Virginia 23508

July 1988

AIRBORNE RADAR TECHNOLOGY FOR WINDSHEAR DETECTION

By

Joseph L. Hibey* and Camille S. Khalaf**

ABSTRACT

The objectives and accomplishments of the two and a half year effort to describe how returns from an on board Doppler radar are to be used to detect the presence of a wind shear are reported. The problem is modeled as one of first passage in terms of state variables, the state estimates are generated by a bank of extended Kalman filters working in parallel, and the decision strategy involves the use of a voting algorithm for a series of likelihood ratio tests. The performance issue for filtering is addressed in terms of error-covariance reduction and filter divergence, and the performance issue for detection is addressed in terms of using a probability measure transformation to derive theoretical expressions for the error probabilities of a false alarm and a miss.

*Associate Professor, Department of Electrical and Computer Engineering, Old Dominion University, Norfolk, Virginia 23529.
**Graduate Research Assistant, Department of Electrical and Computer Engineering, Old Dominion University, Norfolk, Virginia 23529.

TABLE OF CONTENTS

1. INTRODUCTION

We shall begin by briefly summarizing the goals and accomplishments of the two and a half year duration of this grant. Following this overview, we shall present a more detailed exposition and then conclude with some ideas for future work.

The primary objective involved detecting the presence of wind shear and alerting the pilot in time to avoid catastrophe. To accomplish this, we have assumed throughout that a Doppler radar would reside on board the aircraft and provide us with measurements, or returns, that we could then process for purposes of detection and ultimate avoidance. The feasibility of such an approach was indicated in a 1983 report [1] of the National Research Council on wind shear.

With this in mind, work proceeded by first attempting to obtain a mathematical description of the problem. This was achieved by representing the onset of wind shear as a first-passage problem. Also called the classical disruption problem or exit problem, it essentially involves monitoring the evolution of a stochastic process and attempting to determine the first time it exceeds some threshold. The actual models were described in terms of state variables that satisfied a system of stochastic differential equations. The radar returns were represented as nonlinear signals in additive white Gaussian noise. Nonlinear filtering techniques of the extended Kalman type were then applied to estimate both the time of occurrence of wind shear and the magnitude of the so-called microburst. This theoretical formulation and ideas for its simulation and eventual implementation formed the core of the first year and half effort, and is fully described in Ref. [2]; it also served as a progress report for that period and is included in Appendix A to this document.

Encouraged by the preliminary findings of the initial research, we continued in the last year by refining our models to more appropriately reflect reality and by addressing the issue of performance. Thus, we first explicitly took into account phase information and modified the filtering algorithms accordingly. Many computer simulations were run to determine viable approximations leading to acceptable results. We then shifted our attention to the system's overall performance in terms of evaluating the false alarm and miss error probabilities. Although the findings are of a theoretical nature, we shall include some ideas regarding their integration into an actual algorithm.

In the next section we shall formulate the problem in terms of a mathematical model involving state space representations and use nonlinear filtering theory to derive algorithms for estimating the quantitites needed to detect wind shear. Computational issues related to simulation and implementation procedures will then be discussed. Finally, this will lead us to a presentation of detection and performance issues to be followed by some concluding remarks.

Before proceeding, we mention that in the following presentation we shall often refer to paper [2] in Appendix A for notation and some of the basic techniques we have adopted. As will be seen, in some instances the equations used there will not be modified, while in other cases they are. Therefore, for the sake of completeness and ease in reading, if an equation has not changed, it will merely be repeated in this report with the same numbering system and with little or no comment. On the other hand, variants of the original equations will appear in this report with a "prime" symbol attached to the equation number. Finally, starting with Eq. (12) in this report, there are no such corresponding equations in the earlier report.

2. MATHEMATICAL REPRESENTATIONS

Modeling

In [2], we concluded that the radar return can be modeled as

$$r_t = h\,(s_t) + v_t \tag{1}$$

where $h(s_t) = A \sin \{\omega_c + 4\pi\ s_t\ /\ \lambda\}\ t$,

$$s_t = b_t\ z_t + x_t(1-\ z_t) \quad , \tag{2}$$

and

$$z_t = \begin{cases} 0 \quad , & \text{if } t < T \\ 1 \quad , & \text{if } t \geq T \end{cases} \tag{3}$$

This is the classic "signal h (•) in additive white Gaussian noise v" problem. It is somewhat unconventional, however, in that it involves z_t, a zero-one process that distinguishes between the absence of wind shear ($z = 0$ for $t < T$, implying a relatively low wind velocity $s = x$) and the presence of wind shear ($z = 1$ for $t \geq T$, implying a relatively high wind velocity $s = b$). The idea of detection, then, is to derive an estimate $\overline{T}$ of T, the first time of occurrence of a microburst. As such an estimate will require an estimate $\overline{z}$ of z, one must first find state-space models for all the processes involved and then derive an appropriate filter.

The earlier model describing the states has now been modified to include phase information ψ. As usual, we shall assume that ψ is a

uniform random variable distributed over $(-\pi, \pi)$. The resulting model then becomes

$$\text{state:} \quad \begin{bmatrix} dx \\ dz \\ db \\ d\psi \end{bmatrix} = \begin{bmatrix} 0 \\ \lambda \\ 0 \\ 0 \end{bmatrix} dt + \begin{bmatrix} -F & 0 & 0 & 0 \\ 0 & -\lambda & 0 & 0 \\ 0 & 0 & -G & 0 \\ 0 & 0 & 0 & -H \end{bmatrix} \begin{bmatrix} x \\ z \\ b \\ \psi \end{bmatrix} dt + \begin{bmatrix} dW_t \\ dM_t \\ dB_t \\ dU_t \end{bmatrix} \qquad \begin{matrix} (4\text{-a}') \\ (4\text{-b}') \\ (4\text{-c}') \\ (4\text{-d}') \end{matrix}$$

$$\text{observation:} \quad dy_t = A \sin \{\omega_c t + \frac{4 \pi t}{\nu} [b_t z_t + x_t (1-z_t)] + \psi_t\} dt + dV_t \qquad (5')$$

where U_t is Brownian motion (mean zero and variance $U_c t$) that is mutually independent of the above disturbances and initial conditions; with ψ_0 chosen as uniform, H and U_c will typically be selected very small. (Note: in [2], the wavelength ν in (5') was ambiguously written as λ).

Signal Statistics

This new measurement equation involving the process ψ_t can be given the following interpretation. In actuality, at a given range gate there exists a large number of scatterers each with a different velocity. If the sampling rate is sufficiently high, then each of these velocities is approximately constant. Therefore, one can model this situation by imagining one scatterer at each range gate having a velocity that varies with sample time. What is important is that the model possess the same statistics as the real system, and this is accomplished by requiring a uniform distribution for the random phase process ψ_t. Given this model, the filters used to derive the appropriate state estimates will now include additional equations to estimate ψ_t as well.

The signal $h(\cdot)$ can be viewed as an example of exponential modulation

(see, for example, Gray and Davisson [3, pp. 258-260] or Weinstein and Zubakov [4, Chap. 8)), that is,

$$h(t) = \text{Im } q(t) \overset{\Delta}{=} \text{Im } \{A \exp [j(\omega_c t + \frac{4\pi t}{\nu} [b_t z_t + x_t(1-z_t) + \psi)]]\}$$

where Im $\{\cdot\}$ denotes the imaginary part of $\{\cdot\}$. From this, the statistics of h can be derived from those of q. Thus, since the amplitude A has a Rayleigh distribution, the velocity x (or b) has a Gaussian distribution, and the phase ψ has a uniform distribution, it follows that, given z (0 or 1), the sinusoid in h is distributed as $1/\pi\sqrt{1 - y^2}$ for $|y|<1$ (see Papoulis [5, p.100]) and h is Gaussian (see Doviak and Zrnic [6, p. 50]). The results of Doviak and Zrnic [6, p. 440] and Papoulis [5, pp. 268, 269] then lead to an autocorrelation R_q of q of the form

$$R_q(\tau) = c\, e^{-d\tau^2}\, e^{j\omega_c \tau}$$

where c and d are constants, and this implies its power spectrum is Gaussian (also see Doviak and Zrnic [6, p. 43]).

The previous result is valid conditionally, that is, with constants c, d corresponding to x_t when $z_t = 0$ $(t < T)$ and there is no wind shear, and with constants c', d' corresponding to b_t when $z_t = 1$ $(t>T)$ and there is wind shear. To derive an expression valid for all t, one finds through reconditioning and the fact that T is exponentially distributed (see [2] in Appendix A) that R_q is of the form

$$R_q(\tau) = e^{-\lambda t} E\, e^{ja(x_t - x_s)} + (1-e^{-\lambda t})\, E\, e^{ja'(b_t-b_s)} \qquad (6)$$

with a and a' constants. But since the increments $x_t - x_s$ and $b_t - b_s$ are themselves Gaussian, we find as above that

$$R_q(\tau) = e^{-\lambda t}\, c\, e^{-d\tau^2}\, e^{j\omega_c\tau} + (1-e^{-\lambda t})\, c'\, e^{-d'\tau^2}\, e^{j\omega_c\tau} \qquad (7)$$

which shows that q, and therefore h, are nonstationary processes. This result suggests the use of Kalman-type filtering which, unlike Wiener filtering, makes no assumptions regarding the necessity of stationarity.

Filtering

Using this model, we next generate MMSE estimates (denoted with a ^ symbol) of the state variables and use them to detect the onset of wind shear. Thus, as in the earlier report [2], we find that the conditional mean $\hat{z}_t$ given by

$$\hat{z}_t = Pr[t > T \mid y_s,\ 0 < s < t] \qquad (8)$$

represents the probability that wind shear has occurred. But again, recognizing the need for a suboptimal estimate $\bar{z}_t$ because of the nonlinear nature of the problem, a suboptimal estimate $\bar{T}$ of the microburst occurrence time T is given by

$$\bar{T} = \min \{\, t \mid \bar{z}_t > k\} \qquad (9)$$

where k is some threshold in the unit interval. This characterizes our problem as one of first-passage.

Our next step is to specify the filtering algorithms required to generate the estimates used in detection. These will be based on the extended Kalman filter and, for the system in (4') and (5') above, are given as follows:

$$\begin{bmatrix} d\bar{x} \\ d\bar{z} \\ d\bar{b} \\ d\bar{\psi} \end{bmatrix} = \begin{bmatrix} 0 \\ \lambda \\ 0 \\ 0 \end{bmatrix} dt + \begin{bmatrix} -F & 0 & 0 & 0 \\ 0 & -\lambda & 0 & 0 \\ 0 & 0 & -G & 0 \\ 0 & 0 & 0 & -H \end{bmatrix} \begin{bmatrix} \bar{x} \\ \bar{z} \\ \bar{b} \\ \bar{\psi} \end{bmatrix} dt + P \begin{bmatrix} \partial\bar{h}/\partial\bar{x} \\ \partial\bar{h}/\partial\bar{z} \\ \partial\bar{h}/\partial\bar{b} \\ \partial\bar{h}/\partial\bar{\psi} \end{bmatrix} V_c^{-1} \, IN \qquad (10')$$

$$dP = \left\{ \begin{bmatrix} -F & 0 & 0 & 0 \\ 0 & -\lambda & 0 & 0 \\ 0 & 0 & -G & 0 \\ 0 & 0 & 0 & -H \end{bmatrix} P + P \begin{bmatrix} -F & 0 & 0 & 0 \\ 0 & -\lambda & 0 & 0 \\ 0 & 0 & -G & 0 \\ 0 & 0 & 0 & -H \end{bmatrix} + \begin{bmatrix} W_c & 0 & 0 & 0 \\ 0 & \lambda(1-\bar{z}) & 0 & 0 \\ 0 & 0 & B_c & 0 \\ 0 & 0 & 0 & U_c \end{bmatrix} \right.$$

$$\left. - V_c^{-1} P \begin{bmatrix} \partial\bar{h}/\partial\bar{x} \\ \partial\bar{h}/\partial\bar{z} \\ \partial\bar{h}/\partial\bar{b} \\ \partial\bar{h}/\partial\bar{\psi} \end{bmatrix} \begin{bmatrix} \partial\bar{h}/\partial\bar{x} \\ \partial\bar{h}/\partial\bar{z} \\ \partial\bar{h}/\partial\bar{b} \\ \partial\bar{h}/\partial\bar{\psi} \end{bmatrix}^T P \right\} dt - \frac{1}{2} V_c^{-1} \, P \cdot SOT \cdot IN \qquad (11')$$

where $IN \overset{\Delta}{=} dy - (\bar{h} + \frac{1}{2} \cdot SOT)\, dt$, Innovations

$SOT \overset{\Delta}{=} \text{trace}\,[PH]$, Second-Order-Term, and

$H \overset{\Delta}{=} \partial^2 \bar{h} \,/\, \partial\,(\bar{\cdot})^2$, Hessian matrix.

Until now, all we have done is modify the appropriate equations in [2] to account for phase information. Looking ahead, however, to our discussion about performance, it will be helpful to explicitly represent the gain $P\, \partial \bar{h} / \partial (\bar{\cdot})$ in (10') and h above, with $\phi \overset{\Delta}{=} 4\pi / \nu$, as

$$P \begin{bmatrix} \partial\bar{h}/\partial\bar{x} \\ \partial\bar{h}/\partial\bar{z} \\ \partial\bar{h}/\partial\bar{b} \\ \partial\bar{h}/\partial\bar{\psi} \end{bmatrix} \overset{\Delta}{=} \begin{bmatrix} G_x \\ G_z \\ G_b \\ G_\psi \end{bmatrix} \overset{\Delta}{=} \begin{bmatrix} p_{11} & p_{12} & p_{13} & p_{14} \\ p_{21} & p_{22} & p_{23} & p_{24} \\ p_{31} & p_{32} & p_{33} & p_{34} \\ p_{41} & p_{42} & p_{43} & p_{44} \end{bmatrix} \begin{bmatrix} 1 - \bar{z} \\ \bar{b} - \bar{z} \\ \bar{z} \\ (\phi t)^{-1} \end{bmatrix} \phi t\, A \cos\bar{\theta} \tag{12}$$

where

$$h = A \sin \{\omega_c t + \phi t\, [b_t\, z_t + x_t\, (1-z_t)] + \psi_t\} \overset{\Delta}{=} A \sin\theta \quad . \tag{13}$$

Rewriting (10'), we therefore obtain the filter

$$\left.\begin{aligned} d\bar{x} &= -F\, \bar{x}\, dt + G_x\, V_c^{-1} \cdot IN \\ d\bar{z} &= \lambda\, (1-\bar{z})\, dt + G_z\, V_c^{-1} \cdot IN \\ d\bar{b} &= -G\, \bar{b}\, dt + G_b\, V_c^{-1} \cdot IN \\ d\bar{\psi} &= -H\, \bar{\psi}\, dt + G_\psi\, V^{-1} \cdot IN \end{aligned}\right\} \tag{14}$$

3. COMPUTATIONAL ISSUES

The above formulation has been given in germs of continuous time. A discrete-time formulation was derived from this using standard Euler

approximations (see [2]) for purposes of simulation on a digital computer. As was expected, because of the nonlinear nature of the measurement equation given in (5'), the estimates produced by the filters in (10') sometimes diverged for certain choices of parameter such as initial conditions (x_0, b_0, P_0, etc.), noise intensities (W_c, B_c, V_c, etc.), and signal power levels (related to A in (5')). More precisely, the error-covariance matrix P in (11') did not remain nonnegative definite as it should. The reasons why this occurs include the approximation techniques utilized in determining an extended Kalman filter and the finite word length or limited precision of a digital computer; in the latter case, truncation errors tend to accumulate over time (see Jazwinski [7, chap. 9]).

In order to rectify this situation, the following approaches were tried. The diagonal elements of the P matrix in (11') represent error-variances of the appropriate state estimates. Being variances, these should never become negative. Therefore, as a first attempt, these variables were monitored and reset to zero each time they became negative.

With only marginal improvement from the above, we considered the off-diagonal elements of P which represent cross error-covariances. For example, the typical (i,j) element for $i \neq j$ is of the form

$$p_{ij} = E\,(u_i - \hat{u}_i)\,(v_j - \hat{v}_j)$$

where E denotes expectation given the measurements. Using the Schwarz inequality, an upper bound on p_{ij} results in

$$p_{ij} \leq [E(u_i - \hat{u}_i)^2\, E(v_j - \hat{v}_j)^2]^{1/2} = [p_{ii}\, p_{jj}]^{1/2} \quad . \qquad (15)$$

Thus, by monitoring the p_{ij}'s, we were able to reset values to insure the validity of (15) for all time.

Although this approach showed further improvement, it was still not satisfactory. At best, it is an ad hoc technique that works in only limited cases. We therefore turned to square-root filtering algorithms (see, for example, Anderson and Moore [8, chap. 5]). These algorithms are based on so-called singular-value-decompositions and are specifically designed to maintain the nonnegative definite property of P and thereby eliminate filter divergence. Although their use implies a more complex filter, the improvement in the quality of the estimates justifies their adoption. A copy of a computer program that generates state estimates from such a square-root filter of the Kalman type appears in Appendix B with some examples of its output.

Turning now to the implementation aspect of the problem, we refer once again to [2] for the basic methodology. There we see the need for a bank of N of the above type filters each receiving its sample measurements from a particular range location, or range gate, within the region affected by the microburst; each filter will process a batch of M measurements in a serial fashion (the results in Appendix B use M=32), and all filters will work in parallel. The actual decision as to whether or not wind shear has occurred will be based on the outputs $\bar{z}$ of these N filters, and our approach will employ a voting algorithm to be explained in the next section on detection and performance.

4. DETECTION AND PERFORMANCE

The performance issue involves determining how good the filtering and detection algorithms work. In the case of filtering, this is measured by examining the errors in estimation and is directly reflected in the elements

of the error-covariance matrix P in (11'). Whereas this was the subject of the previous section, we now address performance in the context of detection.

A measure of how good a detection scheme works involves an assessment of the errors one commits while making decisions. Here we are confronted with two types of errors: declaring wind shear when it is not present, and declaring no wind shear when indeed it is present. These errors, called false alarm and miss, respectively, are often very difficult to compute. Our objective in this section, then, is to explain how one might evaluate them both theoretically and empirically.

Likelihood-Ratio Test

Our strategy for deciding about the presence or absence of wind shear is based on a likelihood ratio test such as described by Van Trees [9, chap. 2]. As indicated above, we are interested in determining the time at which the process z_t in (3) changes abruptly from zero to one; the detection of such abrupt changes is discussed in the text edited by Basseville and Benveniste [10]. As it turns out, the likelihood ratio involves the estimate $\hat{z}_t$ of z_t given in (8), or, more precisely, its suboptimal estimate $\bar{z}_t$ given in (14). We therefore define the likelihood ratio L as

$$L \overset{\Delta}{=} \frac{\Pr[\text{wind shear} \mid \text{observations of } y \text{ from } 0 \text{ to } t]}{\Pr[\text{no wind shear} \mid \text{observations of } y \text{ from } 0 \text{ to } t]}$$

and use (8) with $\hat{z}$ replaced by $\bar{z}$ to obtain

$$L \overset{\Delta}{=} \frac{\Pr\,[T \leq t \mid y_s,\ 0 \leq s \leq t]}{\Pr\,[T > t \mid y_s,\ 0 \leq s \leq t]} = \frac{\bar{z}}{1-\bar{z}} \quad . \tag{16}$$

The likelihood-ratio-test (LRT) involves testing the magnitude of L in relation to some threshold γ' defined as

$$\gamma' \overset{\Delta}{=} \frac{P_0\,(C_{10}-C_{00})}{P_1\,(C_{01}-C_{11})} \tag{17}$$

where P_0 and P_1 are the a priori probabilities of the absence and presence of wind shear, respectively, and C_{ij}, i,j = 0,1 are the relative costs of making correct (i=j) and incorrect ($i \neq j$) decisions. For example, as is often the case, if no cost is attached to making correct decisions, $C_{00} = C_{11}$ = 0; a choice of C_{10} = 3, say, implies a cost of deciding in favor of wind shear (i=1) when indeed there is none (j=0), while a cost of C_{01} = 19, say, is incurred in deciding against wind shear (i=0) when in fact it is present (j=1). Also, by way of example, P_0 = .95 indicates a strong belief that no wind shear is present and therefore implies P_1 = .05. The actual values used in any test will be chosen by the pilot based on airline safety procedures and standards, and current weather reports. From the choices selected above, the interpretation is that one is less tolerant of missing a wind shear ($C_{01} > C_{10}$) in a situation where wind shear appears to be unlikely ($P_0 >> P_1$). We therefore arrive at the following LRT:

$$\text{LRT:} \quad \frac{\bar{z}}{1-\bar{z}} \underset{H_0}{\overset{H_1}{\gtrless}} \gamma' \quad . \tag{18}$$

Here, H_0 denotes the hypothesis there is no wind shear and H_1 denotes the hypothesis there is wind shear. Equivalently, assuming $\gamma' > 0$, we have

$$\text{LRT:} \quad \bar{z} \underset{H_0}{\overset{H_1}{\gtrless}} \gamma \tag{19}$$

where $\gamma \overset{\Delta}{=} \gamma' / (1+\gamma')$. Thus, we compute $\bar{z}$ and declare the presence of wind shear if $\bar{z} > \gamma$, and declare its absence otherwise.

Voting Algorithm

We next recall that in reality we have a bank of N filters each using measurements taken at a specific range gate. Therefore, we will need N LRT's and some type of voting algorithm on which to base our decision. We proceed as follows.

Let us assume a symmetric microburst pattern and, for convenience, N + 1 filters acting over a range that encloses the resolution volume of the weather target, as shown below:

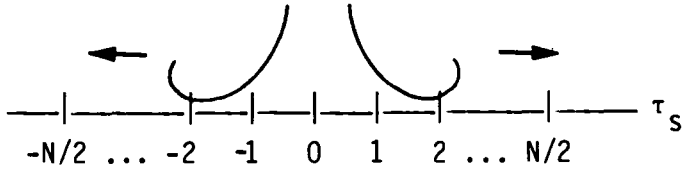

Here, range time $\tau_s \overset{\Delta}{=} n\,\Delta\tau$, $n = -N/2, \ldots, -1, 0, 1, \ldots, N/2$; also see Fig. 3 in [2]. We further assume that if, say, 4/5 of the tests indicate

wind shear (H_1), we declare wind shear; if 4/5 of the tests indicate no wind shear (H_0), we declare no wind shear; otherwise, we make no decision at this time and wait for more data. To express this, we first denote the indicator function $I\{.\}$ of an event A by

$$I\{A\} = \begin{cases} 1 & \text{if A occurs} \\ 0 & \text{otherwise} \end{cases} .$$

We next define the number J of "triggered gates" (those indicating wind shear) by

$$J \overset{\Delta}{=} \sum_{i=-N/2}^{N/2} I[\bar{z}_t\ (i\Delta\tau) > \gamma] \tag{20}$$

and its complement by $\bar{J} \overset{\Delta}{=} (N+1-J)$ (the number of gates indicating no wind shear). Then, setting the ratio r = 4/5, our voting algorithm becomes

$$\left.\begin{array}{l} \text{if } J > r\ (N+1), \text{ then decide } H_1; \\ \text{if } \bar{J} > r\ (N+1), \text{ then decide } H_0; \\ \text{otherwise, make no decision.} \end{array}\right\} \tag{21}$$

The ratio r used in (21) is a design parameter set by the pilot in accordance with weather reports and existing standards and guidelines. For example, with a weather report indicating virtually no winds, 4/5 might be viable because any microburst would probably be symmetric; on the other hand, a report of a 20 knot wind might suggest the use of ratio 2/3 because any microburst would probably be asymmetric. In general, as weather reports indicate higher wind velocities, a lower number of "gates" need to be "triggered" before declaring the presence of wind shear because its occurrence becomes more probable. Finally, we note that $\bar{z}$ is a process evolving with time t, so any meaningful test would actually require that

(21) give consistent results over some prespecified duration of time before the ultimate decision is made; examining $\bar{b}_t$ over this duration would also provide a direct correlation with this decision.

Error Analysis

Referring to (19), we see that a so-called type 1 error or false alarm is committed if hypothesis H_0 (no wind shear) is indeed true, yet we mistakenly conclude that hypothesis H_1 (wind shear) is true because $\bar{z} > \gamma$. Likewise a so-called type 2 error or miss is committed if H_1 is true, yet we decide in favor of H_0 because $\bar{z} < \gamma$. Therefore, denoting the conditional densities of $\bar{z}$ by $p(\bar{z}|H_i)$, i=0, 1, we define the error probabilities of a false alarm P_F and miss P_M by

$$P_F \overset{\Delta}{=} \Pr[\bar{z}_t > \gamma \mid H_0] = \int_{\gamma}^{1} p(\bar{z}_t \mid H_0)\, d\,\bar{z}_t \tag{22}$$

$$P_M \overset{\Delta}{=} \Pr[\bar{z}_t < \gamma \mid H_1] = \int_{0}^{\gamma} p(\bar{z}_t \mid H_1)\, d\,\bar{z}_t \quad . \tag{23}$$

One approach to computing P_F and P_M is to use Monte Carlo techniques. For example, considering P_F (similar remarks apply to P_M), one would generate observations from (5'), but with $z_t = 0$ which corresponds to H_0 being true as in (22). The observations would then be used in (10') and (11') to evaluate $\bar{z}_t$, and finally P_F could be evaluated using relative frequency type calculations.

On the other hand, (22) and (23) show the need to evaluate the conditional densities $p(\bar{z} \mid H_i)$, i=0, 1 of the likelihood ratio $\bar{z}$, but quite

often this is not possible. In such cases we might be satisfied with obtaining, for example, upper bounds on these error probabilities as in [11]. Although we shall not follow that approach here, some of the ideas in [11] will be used to derive theoretical expressions for P_F and P_M. If they could then be evaluated, their values could be compared with the empirical values obtained from the Monte Carlo techniques mentioned above. We now proceed with our analysis of P_F defined in (22); similar comments apply to P_M in (23) and, for most part, will be omitted.

Our approach can be summarized as follows. If $\bar{z}_t$ of (10') were an optimal estimate of z_t rather than a suboptimal estimate, then the innovations process IN driving (10') would be a Brownian motion process and the density $p(\bar{z})$ of $\bar{z}_t$ would satisfy the Fokker-Planck (FP) equation

$$\frac{\partial P(\bar{z})}{\partial t} = -\frac{\partial}{\partial \bar{z}}\left[\lambda(1-\bar{z})\ p(\bar{z})\right] + \frac{1}{2}\frac{\partial^2}{\partial z^2}\left[(G_z\ V_c^{-1})^2\ p(\bar{z})\right]\ ; \qquad (24)$$

this is also called the Kolmogorov forward equation. However, this equation does not exist because $\bar{z}_t$ is in fact a suboptimal estimate of z_t, so IN is not Brownian motion. Furthermore, (22) requires the conditional density $p(\bar{z} \mid H_0)$, not the unconditional density satisfying (24) which has coefficients $\lambda(1-\bar{z})$ and $G_z\ V_c^{-1}$ that are the same regardless of which hypothesis is true. For these reasons, therefore, we shall use a measure transformation (see [11] and [12] for a similar application) which will lead to a FP equation with coefficients that do indeed distinguish between the two hypotheses. The cost, however, will be an increase in the dimension of

the states whose density satisfies this equation, so the conditional density required in (22) will follow by integration.

To begin the derivation, we define the martingale

$$m_t \overset{\Delta}{=} \int_0^t f(\bar{h}) \, [dy_\tau - h_\tau \, d\tau] \tag{25}$$

where $f(\bar{h})$ will be specified shortly. Then defining the exponential formula (see van Schuppen [13, pp. 32, 33] or Brêmaud [14, pp. 336-338])

$$\varepsilon(m_t) \overset{\Delta}{=} \exp \left[m_t - \int_0^t f^2(\bar{h}) \, V_c \, d\tau \right]$$

$$= \exp \left\{ \int_0^t f(\bar{h}) \, [dy - h \, d\tau] - \int_0^t f^2(\bar{h}) \, V_c \, d\tau \right\} \tag{26}$$

it follows that if $E \, \varepsilon(m_T) = 1$, then $\varepsilon(m_t)$ can be used with the original probability measure P_0 corresponding to H_0 to define a new probability measure P_2 (see van Schuppen [13, p. 38] or Lipster and Shiryayev [15, pp. 314, 315]) such that

$$\varepsilon(m_t) = dP_2 / dP_0 \quad . \tag{27}$$

The verification that $E \, \varepsilon(m_T) = 1$ follows from van Schuppen [13, pp. 34-36] or Lipster and Shiryayev [15, p. 295] by invoking a sufficient condition requiring that $f^2(\bar{h})$ be bounded; thus choosing $f(\bar{h}) = \bar{h} V_c^{-1}$ satisfies the requirement because $\bar{h}$ is a sinusoid bounded by 1. Turning once again to van

Schuppen [13, pp. 40-42], we use the martingale translation theorem to obtain a measurement equation with respect to the new measure P_2 given by

$$dy = h\,dt + \bar{h}\,dt + dM \tag{28}$$

where the martingale M is a Brownian motion process; for a proof of this last assertion, see [16, p. 53] for a similar derivation. Finally, we use (28) in (14) to obtain the new filtering equations

$$\left.\begin{aligned}
d\bar{x} &= [-F\,\bar{x} + G_x\,V_c^{-1}\,h]\,dt + G_x\,V_c^{-1}\,dM \\
d\bar{z} &= [\lambda(1-\bar{z}) + G_z\,V_c^{-1}\,h]\,dt + G_z\,V_c^{-1}\,dM \\
d\bar{b} &= [-G\bar{b} + G_b\,V_c^{-1}\,h]\,dt + G_b\,V_c^{-1}\,dM \\
d\bar{\psi} &= [-H\,\bar{\psi} + G_\psi\,V_c^{-1}\,h]\,dt + G_\psi\,V_c^{-1}\,dM
\end{aligned}\right\} . \tag{29}$$

As (29) indicates, the "drift" coefficients now explicitly contain the signal h of (13) and, since h depends explicitly on z, these coefficients can distinguish between the hypotheses H_0 and H_1 as z goes from 0 to 1, respectively. However, because our interest is currently focused on evaluating P_F, we set z = 0 and express h by

$$h = A \sin\{\omega_c t + \phi_t\,x_t + \psi_t\} \overset{\Delta}{=} A \sin\theta_0 \quad . \tag{30}$$

Therefore, substituting (30) into (29) indicates that the filter in (29) represents a coupling of not only the state estimates $\bar{x}$, $\bar{z}$, $\bar{b}$, and $\bar{\psi}$, but also of the original (unfiltered) states x of (4-a') and ψ of (4-d'). This

then is the anticipated increase in dimension alluded to above and leads to the following augmented system of equations:

$$\left.\begin{aligned} d\bar{x} &= [-F\bar{x} + G_x V_c^{-1} h]\, dt + G_x V_c^{-1} dM \\ d\bar{z} &= [\lambda(1-\bar{z}) + G_z V_c^{-1} h]\, dt + G_z V_c^{-1} dM \\ d\bar{b} &= [-G\bar{b} + G_b V_c^{-1} h]\, dt + G_b V_c^{-1} dM \\ d\bar{\psi} &= [-H\bar{\psi} + G_\psi V_c^{-1} h]\, dt + G_\psi V_c^{-1} dM \\ dx &= -F x\, dt + d W \\ d\psi &= -H \psi\, dt + d U \end{aligned}\right\} . \tag{31}$$

This can also be expressed in vector form by defining the augmented state as $\underline{x} \overset{\Delta}{=} [\bar{x}\ \bar{z}\ \bar{b}\ \bar{\psi}\ x\ \psi]^T$ and writing

$$d\underline{x} = A(\underline{x}, t)\, dt + B(\underline{x}, t)\, d\underline{W} \tag{32}$$

where the column vectors $A(\underline{x},t)$, $B(\underline{x},t)$ and $\underline{W}$ are defined accordingly.

We now recall that our objective was to obtain an expression for $p(\bar{z}_t \mid H_0)$ as required by (22). Therefore, using h of (30) in (32), the conditional joint density of $\underline{x}$ given H_0, denoted by $p(\underline{x}, t \mid H_0)$, satisfies the Fokker-Planck equation

$$\frac{\partial p}{\partial t} = -\nabla_{\underline{x}} \cdot (Ap) + \frac{1}{2} \sum_{i,j=1}^{6} \frac{\partial^2 (b_{ij} p)}{\partial x_i\, \partial x_j} . \tag{33}$$

where $\nabla_{\underline{x}}$ denotes the gradient operator with respect to the vector $\underline{x}$ and $b_{ij} \overset{\Delta}{=} (B B^T)_{ij}$. The fact that (33) is valid follows from our use of the

measure transformation that resulted in the state equation (32) being driven by a Brownian motion process $\underline{W}$. The density $p(\bar{z}_t \mid H_0)$ now follows from integrating $p(\underline{x}, t \mid H_0)$, that is,

$$p(\bar{z}_t \mid H_0) = \int_{-\infty}^{\infty} d\bar{x} \int_{-\infty}^{\infty} d\bar{b} \int_{-\pi}^{\pi} d\bar{\psi} \int_{-\infty}^{\infty} dx \int_{-\pi}^{\pi} d\psi \; p(\underline{x}(t) \mid H_0) \quad , \qquad (34)$$

and the final expression for the probability of a false alarm defined in (22) becomes

$$P_F = \int_{\gamma}^{1} d\bar{z} \int p(\underline{x}, t \mid H_0) \, d(\bar{x}, \bar{b}, \bar{\psi}, x, \psi) \qquad (35)$$

where the latter integration symbol denotes the multiple integration shown explicitly in (34).

A similar analysis leads to an expression for the probability of a miss P_M. To derive it, we set $z = 1$ in (13) and express h by

$$h = A \sin \{\omega_c t + \phi t \, b_t + \psi_t\} \overset{\Delta}{=} A \sin \theta_1 \; . \qquad (36)$$

Its use in (29) then represents a filter with coupling among the states $\bar{x}$, $\bar{z}$, $\bar{b}$, and $\bar{\psi}$, and also the states b of (4-c') and ψ of (4-d'). Therefore, the equation for x in (31) is replaced by the equation for b and the augmented state vector becomes $\underline{x} = [\bar{x} \; \bar{z} \; \bar{b} \; \bar{\psi} \; b \; \psi]^T$. The vectors A and B of (32) change accordingly, and (34) is replaced by

$$p(\bar{z}_t \mid H_1) = \int_{-\infty}^{\infty} d\bar{x} \int_{-\infty}^{\infty} d\bar{b} \int_{-\pi}^{\pi} d\bar{\psi} \int_{-\infty}^{\infty} db \int_{-\pi}^{\pi} d\psi \; p(\underline{x}, t \mid H_1). \quad (37)$$

Then the final expression for the probability of a miss defined in (23) becomes

$$P_M = \int_0^{\gamma} d\bar{z} \int p(\underline{x}, t \mid H_1) \, d(\bar{x}, \bar{b}, \bar{\psi}, b, \psi) \quad (38)$$

To summarize what we have done, the false alarm error probability P_F and miss error probability P_M each require the solution of the Fokker-Planck equation of (33) followed by the integrations in (35) and (38), respectively. Since an exact solution is virtually impossible, some numerical procedure must be used to obtain suitable approximations. Considering a worst case scenario, however, by assuming large measurement noise such that $V_c^{-1} \to 0$), causes many terms in A and B to vanish and thereby makes (33) less formidable.

5. CONCLUSIONS

From the outset, we proposed to describe how one might process the returns from an on board Doppler radar system so as to detect the presence of a wind shear. Questions relating to specific hardware such as antenna design and so on were not the major concern. In contrast, the scope of this effort was to address software issues in the context of deriving filtering and detection algorithms to achieve the above objective.

That this is a final report should in no way suggest the completion of this phase of the overall effort. A good part of the preceding formulation

has resulted in theoretical type expressions which ideally could be used as a basis for practical implementation, and we have endeavored to indicate this in the appropriate places of this report. It is our sincerest hope that the adoption of some of these ideas will be useful in the attempt to further understand and ultimately solve the wind shear problem.

ACKNOWLEDGEMENT

This is a final report on the research project "Airborne Radar Technology for Windshear Detection." Specific efforts were directed in the area of "Wind Shear Modeling and Detection: An Analysis in Terms of a First-Passage Problem." The performance period for this research ended August 31, 1988. This work was supported by the NASA Langley Research Center through NASA Research Grant NAG-1-626 and was monitored by Dr. Leo D. Staton, Technical Monitor of the GCD-Antenna & Microwave Research Branch, NASA Langley Research Center, MS/490.

REFERENCES

1. National Research Council, Report of the Committee on Low-Attitude Wind Shear and its Hazard to Aviation, National Academy Press, Washington, D.C., 1983.

2. C. S. Khalaf, J. L. Hibey, and L. D. Staton, "Wind Shear Modeling and Detection: An Analysis in Terms of a First-Passage Problem, presented at the Twentieth Asilomar Conference on Signals, Systems, and Computers, Pacific Grove, CA., Nov. 1986.

3. R. M. Gray and L. D. Davisson, Random Processes: A Mathematical Approach for Engineers, Prentice-Hall, 1986.

4. L. A. Wainstein and V. D. Zubakov, Extraction of Signals from Noise, Prentice-Hall, 1962.

5. A. Papoulis, Probability, Random Variables and Stochastic Processes, McGraw-Hill, 1984.

6. R. J. Doviak and D. S. Zrnic, Doppler Radar and Weather Observations, Academic Press, 1984.

7. A. H. Jazwinski, Stochastic Processes and Filtering Theory, Academic Press, 1970.

8. B. D. Anderson and J. B. Moore, Optimal Filtering, Prentice-Hall, 1979.

9. H. L. Van Trees, Detection, Estimation, and Modulation Theory, Part I, Wiley, 1968.

10. M. Basseville and A. Benveniste (ed.), Detection of Abrupt Changes in Signals and Dynamical Systems, Springer-Verlag, 1980.

11. J. L. Hibey, D. L. Snyder, and J. H. van Schuppen, "Error Probability Bounds for Continuous-Time Decision Problems," IEEE Trans. on Information Theory, Vol. IT-24, No. 5, Sept. 1978, pp. 608-622.

12. J. L. Hibey, "Cycle Slipping in an Optical Communication System Employing Subcarrier Angle Modulation," IEEE Trans. on Information Theory, Vol. IT-33, No. 2, Mar. 1987, pp. 203-209.

13. J. H. van Schuppen, "Estimation Theory for Continuous Time Processes, a Martingale Approach," Ph.D. Dissertation, Univ. of Calif., Berkeley, 1973.

14. P. Brémaud, Point Processes and Queues: Martingale Dynamics, Springer-Verlag, 1981.

15. R. S. Lipster and A. N. Shiryayev, Statistics of Random Processes II, Applications, Springer-Verlag, 1978.

16. J. L. Hibey, "Error-Probability Bounds for Continuous-Time Decision Processes," D.Sc. Dissertation, Washington University, St. Louis, 1976.

APPENDIX A

DEPARTMENT OF ELECTRICAL & COMPUTER ENGINEERING
COLLEGE OF ENGINEERING & TECHNOLOGY
OLD DOMINION UNIVERSITY
NORFOLK, VIRGINIA 23508

WIND SHEAR MODELING AND DETECTION: AN ANALYSIS IN TERMS OF A FIRST-PASSAGE PROBLEM

By

C. C. Khalaf

and

J. L. Hibey, Principal Investigator

Progress Report
For the period ending November 30, 1986

Prepared for the
National Aeronautics and Space Administration
Langley Research Center
Hampton, Virginia 23665

Under
NASA Grant NAG-626
Dr. Leo Staton
FED-Antenna & Microwave Research Branch

Submitted by the
Old Dominion University Research Foundation
P. O. Box 6369
Norfolk, VA 23508

January 1987

WIND SHEAR MODELING AND DETECTION: AN ANALYSIS IN TERMS OF A FIRST-PASSAGE PROBLEM

By

C. S. Khalaf[1] and J. L. Hibey[2]

SUMMARY

The enclosed manuscript was presented at the Proceedings of the 1986 Asilomar Conference on Signals, Systems, and Computers, which was held in Pacific Grove, California, in November 1986.

The project work is supported by NASA Grant NAG-1-626.

---

[1] Graduate Research Assistant, Department of Electrical & Computer Engineering, Old Dominion University Research Foundation, Norfolk, VA 23508.

[2] Associate Professor, Department of Electrical & Computer Engineering, Old Dominion University Research Foundation, Norfolk, VA 23508.

WIND SHEAR MODELING AND DETECTION: AN ANALYSIS IN TERMS OF A FIRST-PASSAGE PROBLEM

C. S. Khalaf*, J. L. Hibey* and L. D. Staton**

* Old Dominion University, Norfolk, Virginia

** MS 490 NASA Langley Research Center, Hampton, Virginia

ABSTRACT

An approach is proposed for extracting information from airborne Doppler radar returns that can be used to determine the presence of wind shear in commercial aviation. Issues that are discussed include modeling in terms of stochastic differential equations, estimation in terms of minimummean-square-error filters, and detection in terms of a first passage problem. Some discussion of the hardware architecture needed to process the data in a timely and efficient manner is also included

1 INTRODUCTION

The problem of wind shear in commercial aviation has always existed, but only recently has it been given the attention it deserves In the last fifteen years, it has been listed as the cause of several accidents involving large carriers, with the most recent being the crash of Delta Airlines Flight 191 in Dallas on August 2, 1985 that claimed the lives of 137 people

The phenomenon can be loosely described as a sudden downburst of wind at a velocity of approximately 40 meters/second which, upon impact with the ground, results in a horizontal component of wind velocity with high magnitude, and with direction that abruptly changes as one moves through it at an altitude close to the ground. Thus it poses a severe hazard to aircraft who encounter this so-called microburst (see Fujita [1]) in either the take-off or landing phase of flight, in that the aircraft first experiences a high head wind causing lift followed suddenly by a high tail wind causing descent. Therefore, with little altitude in which to maneuver, pilots are unable to recover control and disaster results

The many causes of wind shear are discussed in report [2], also see Doviak and Zrnic [3,chap 9] These range from wet microbursts that occur in the wake of thunderstorms to dry microbursts that occur in more tranquil climatic conditions. Research in this area continues to gain a better understanding of the physics involved.

The above report also discusses various methods for detecting the presence of wind shear and alerting the pilot in a timely fashion Among these is the use of ground based radars such as the system called NEXPAD, a planned network of Doppler radars to be operated by the National Weather Service, and a proposed Doppler radar system called TDWR that would be placed specifically at principal airports. The report also proposes the use of airborne Doppler radars, and it is this topic that we wish to explore in this paper

To be more precise, we shall propose a method for extracting information from Doppler radar returns that can be used to determine the presence of wind shear. Issues to be discussed will include modeling in terms of stochastic differential equations, estimation in terms of minimum-mean-square-error (MMSE) filters, and detection in terms of a first-passage problem. In addition, we shall include some discussion of the hardware architecture needed to process the data in a timely and efficient manner.

2. MATHEMATICAL DESCRIPTION

The method of solution we shall investigate is based on the classical disruption problem In the mathematics literature, this is sometimes called the first-passage problem or the exit problem. More precisely, one monitors the evolution of a stochastic process and attempts to determine the first time the process reaches a boundary or exceeds a threshold. In terms of detecting wind shear, the first time the threshold is exceeded will correspond to the onset of a microburst. Our formulation will be based on a paper by Davis [4] who shows how nonlinear filtering techniques can be useful in the detection process. We now proceed to describe the radar signal returns, the state space model, and the filtering and detection algorithm.

Radar Signal Returns

The radar signals used in weather applications are composites of signals from a very large number of scatterers (e.g., hydrometeors) each of which can be considered a point target, collectively they describe a so-called distributed target. After the round trip propagation delay, echoes due to one pulse are continuously received over a time interval equal to twice the time it takes the pulse to propagate across the volume containing

the scatterers The echoes can be expressed as (see, e g , Van Trees [5])

$$r(\tau_s) = r(2r_v/c) = \frac{1}{\sqrt{2}}[\sum_i A_i W_i e^{-4\pi r_i/\lambda}]e^{-j4\pi r_v/\lambda}$$

where $\tau_s = 2r_v/c$ is the so-called range time, r_v is the range resolution volume, r_i is the incremental range within the volume, $|A_i|/\sqrt{2}$ is the echo amplitude of the i^{th} scatterer located at range $r_v + r_i$, and W_i is the corresponding range weighting function For a short pulse duration, however, this equation does not contain any Doppler shift information because weather targets move at relatively slow speed (r_i is constant during the time scatterer i is illuminated by the pulse). Therefore, in order to include Doppler shift information needed for wind shear analysis, one would have to look at returns from a number of pulses where each return is of the above form and consists of reflections at a number of range gates. By proper sampling, then, a sequence of complex video samples $r(kT_s)$ separated by the pulse repetition time T_s can be obtained for each and every range gate This sequence would consist of a signal in additive noise, i e ,

$$r(kT_s) = S_k e^{j\omega_d k T_s} + V_k, \quad k = 0,1, \quad ,M-1$$

where ω_d is the Doppler shift and M is the number of returns considered at one time. The fundamental difference between these equations is that the former describes the reflection process in space (range time) while the latter describes it in time (sample time) at one specific range Because our analysis will be based on the sample time sequences that contain the Doppler shift information, the use of dynamical models that incur abrupt changes are natural candidates for wind shear applications

State Space Model

In view of the above discussion let us assume that the radar return can be modeled as

$$r_t = h(s_t) + v_t \qquad (1)$$

where $h(s_t) = A \sin(\omega_c + 4\pi s_t/\lambda)t$,
A = amplitude (envelope),
s_t = radial velocity (along the radar's beam axis),
v_t = Gaussian white noise with zero mean and correlation matrix V_c,
ω_c = carrier frequency, and
λ = wavelength

We are thus assuming a phase modulation format where each measurement r_t represents a return at some fixed range gate, other formats might also be applicable More precisely, consider the following figure denoting radar returns from sequential pulses of pulse repetition time T_s and round trip propagation time τ_s as defined above

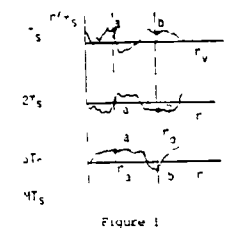

Figure 1

The sequence of M points {a} denotes samples of the scattered signal at some distance r_a in the entire volume, {b} denotes samples at distance r_b, etc Imagine, for example, that each return is separated by T_s = 0 1 ms arising from an assumed microburst of 15 km in depth These various sequences can be used to generate statistics for s_t at the corresponding ranges r_v within the microburst. For example, one could use all M samples in a batch mode to compute the radial velocity with a resolution $(\lambda/2)(1/MT_s)$, where λ is the radar carrier wavelength; either FFT or covariance methods could be used.

Now suppose one wishes to estimate the occurrence of the abrupt change in the velocity s_t that accompanies a microburst. Consider the following figure

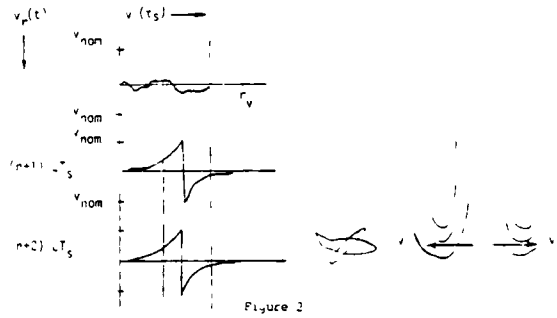

Figure 2

Here we have shown that, in a microburst, the downburst impacts the ground and the magnitude of the velocity v changes abruptly from zero at the center of the microburst to some relatively large nominal value $\pm v_{nom}$, in the absence of a microburst, the magnitude and direction of v are random

To formulate a state space model for the above situation, let us imagine that before the microburst, the velocity is a stochastic process x_t whose mean is a relatively small nonzero constant and whose variance is a relatively large constant; after the microburst, we shall imagine that the velocity is a stochastic process b_t whose mean is a relatively large constant (corresponding to v_{nom}) and whose variance is relatively small. Thus we can write

$$s_t = b_t z_t + x_t (1-z_t) \qquad (2)$$

where

$$z_t = \begin{cases} 0 & \text{if } t < T \\ 1 & \text{if } t \geq T \end{cases} \qquad (3)$$

and T denotes the random time of occurrence of the microburst. If we now assume that T is an exponentially distributed random variable with parameter λ, and redefine the observations r_t in (1) as $dy_t = r_t dt$, then a possible model might be

$$\text{state} \quad \begin{bmatrix} dx \\ dz \\ db \end{bmatrix} = \begin{bmatrix} 0 \\ \lambda \\ 0 \end{bmatrix} dt + \begin{bmatrix} -F & 0 & 0 \\ 0 & -\lambda & 0 \\ 0 & 0 & -G \end{bmatrix} \begin{bmatrix} x \\ z \\ b \end{bmatrix} dt + \begin{bmatrix} dW_t \\ dM_t \\ dB_t \end{bmatrix} \qquad \begin{matrix} (4\text{-a}) \\ (4\text{-b}) \\ (4\text{-c}) \end{matrix}$$

$$\text{observation} \quad dy_t = A \sin(\omega_c + 4\pi f b_t z_t + x_t(1-z_t)^{1/\lambda})t + dV_t \qquad (5)$$

where W_t = Brownian motion (mean zero and variance $W_c t$),

M_t = martingale associated with a Poisson process z_t stopped at its first jump time,

B_t = Brownian motion (mean zero and variance $B_c t$),

V_t = Brownian motion (mean zero and variance $V_c t$), and

all Brownian motions and initial conditions are mutually independent.

The parameters F and G must be chosen to achieve the desired statistical properties mentioned above and, at the same time, must guarantee stable solutions when their discrete approximations are implemented on a digital computer. The stability issue will be discussed later in the section on simulation. Considering the statistical properties required of x_t, its solution, with x_o assumed deterministic, implies the following mean and variance:

$$Ex_t = e^{-Ft}x_o, \quad \text{var } x_t = (W_c/2F)(1-e^{-2Ft})$$

Since in reality we are unable to have $t \to \infty$ to obtain a large constant variance, we shall choose F to be relatively large (and W_c even larger). However, such a choice drives the mean to zero, which is not desired. Therefore, to compensate for this, the x_t used in (5) will actually be the x_t from (4-a) plus a constant nominal value of x_{nom}. On the other hand, since the b_t process has a mean and variance with the same form as that for x_t, and the desired statistical properties of b_t are opposite those of x_t, we choose G to be relatively small.

Filtering and Detection Algorithm

Using the state and observation equations in (4) and (5) above, we can generate MMSE estimates $\hat{x}$, $\hat{z}$, and $\hat{b}$ of the respective states x, z, and b and use them to detect the onset of wind shear. More specifically, recalling the definition of z_t in (3), it turns out that

$$\hat{z}_t = \Pr[t \geq T | y_s,\ 0 \leq s \leq t] \qquad (6)$$

i.e., the conditional mean $\hat{z}_t$ is precisely the probability that wind shear has occurred. However, because our model represents a system of nonlinear stochastic differential equations, it is not possible to derive the optimal estimate $\hat{z}$ in terms of a finite-dimensional realization. Therefore, this so-called moment closure problem compels us to seek a suboptimal filter. Once specified, then we can use the suboptimal estimate $\bar{z}_t$ of z_t to generate an estimate $\bar{T}$ of T, the first time of occurrence of a microburst, by choosing some threshold $k \in (0,1)$ and setting

$$\bar{T} = \min\{t | \bar{z}_t \geq k\} \qquad (7)$$

It is the form of (7) that causes us to describe the problem as one of first-passage. Its successful use as a detection algorithm will depend heavily on the quality of the estimates of z provided by the filter, the k parameter is also important in that it is related to the performance issue and the concomitant false-alarm and miss error-probabilities. With this in mind, we have opted to compare the use of the extended Kalman filter (EKF) with the truncated second order filter (TSOF) as presented, for example, by Jazwinski [6,chap 9]. A slight modification in the error-covariance equations, however, is required because of the martingale M_t in (4-b) associated with the purely discontinuous process z_t. In any case, with overbars denoting suboptimal estimates and P denoting the error-covariance matrix, we have the following:

$$\begin{bmatrix} d\bar{x} \\ d\bar{z} \\ d\bar{b} \end{bmatrix} = \begin{bmatrix} 0 \\ \lambda \\ 0 \end{bmatrix} dt + \begin{bmatrix} -F & 0 & 0 \\ 0 & -\lambda & 0 \\ 0 & 0 & -G \end{bmatrix} \begin{bmatrix} \bar{x} \\ \bar{z} \\ \bar{b} \end{bmatrix} dt + P \begin{bmatrix} \partial\bar{h}/\partial\bar{x} \\ \partial\bar{h}/\partial\bar{z} \\ \partial\bar{h}/\partial\bar{b} \end{bmatrix} V_c^{-1} \cdot IN \qquad (8)$$

$$dP = \left\{ \begin{bmatrix} -F & 0 & 0 \\ 0 & -\lambda & 0 \\ 0 & 0 & -G \end{bmatrix} P + P \begin{bmatrix} -F & 0 & 0 \\ 0 & -\lambda & 0 \\ 0 & 0 & -G \end{bmatrix} + \begin{bmatrix} W_c & 0 & 0 \\ 0 & \lambda(1-\bar{z}) & 0 \\ 0 & 0 & B_c \end{bmatrix} - V_c^{-1} P \begin{bmatrix} \partial\bar{h}/\partial\bar{x} \\ \partial\bar{h}/\partial\bar{z} \\ \partial\bar{h}/\partial\bar{b} \end{bmatrix} \begin{bmatrix} \partial\bar{h}/\partial\bar{x} \\ \partial\bar{h}/\partial\bar{z} \\ \partial\bar{h}/\partial\bar{b} \end{bmatrix}^T P \right\} dt - \frac{1}{2} V_c^{-1} P \cdot SOT \cdot IN \qquad (9)$$

where $IN \triangleq dy - (\bar{h} + \frac{1}{2} \cdot SOT)dt$, innovations

$SOT \triangleq \text{trace}[PH]$, second-order-term, and

$H \triangleq \partial^2\bar{h}/\partial(\bar{\cdot})^2$, Hessian matrix.

In deriving these equations, use is made of the fact that the definition of z_t in (3) implies $z_t^2 = z_t$. Also the term $\lambda(1-\bar{z})$ in the error-covariance equation is a result of the quadratic variation of the martingale M_t in (4-b). Finally note that if the term SOT is zero, then the preceding equations define the EKF; otherwise, they define the TSOF.

3 SIMULATION

The approach used in discretizing the continuous-time equations given in the previous section is based on Euler's approximation, see, for example, Franklin and Powell [7, ch 3]. Since

the equations in (4) are decoupled, we can illustrate the approach by discretizing (4-a) to obtain

$$x_{k+1} = (1 - F\Delta)x_k + w_k\Delta$$

where w_k is a zero-mean Gaussian white noise sequence with correlation matrix W_c. To be stable, one requires that $|1-F\Delta|<1$, i.e., $0 < F < 2/\Delta$ for a sampling interval of length Δ which, for us, has been chosen to be 1. Analogous statements hold for (4-c). Therefore, recalling the discussion on parameter selection in the previous section on state-space models, we choose $F \approx 1.90$ and $G \approx .01$.

The results obtained thus far from computer simulations have been encouraging and lead us to conclude that the overall approach is a sound one. As is so often the case in such simulations, care must be taken in selecting values of state and observation noise statistics and initial error-covariances to prevent filter divergence, and we are continuing to investigate adaptive techniques to remedy this problem. However, in those cases where the filtered estimates did converge, the decision that wind shear had occurred was made within a few sampling intervals of the actual occurrence. It is anticipated that a complete presentation of these simulations will be forthcoming in the near future.

We also plan to simulate microbursts through the use of a model based on the fluid continuity equation

$$\nabla \cdot (\rho v) = 0$$

with vertical hydrostatic equilibrium. Assumptions include inviscid flow with no heat input (dry microburst). An azimuthally symmetric solution in cylindrical coordinates, with v_z and v_r denoting vertical and radial velocity components, respectively, is

$$v_z = \frac{bc}{1+bH} e^{-r^2/2A^2}(e^{-z/b} - e^{-Hz})$$

$$v_r = \frac{2A^2c}{2} \frac{1 - e^{-r^2/2A^2}}{r} e^{-z/b}$$

Here, H is the actual scale height, A is the initial radius at the top of the column, c is the initial velocity or strength, and b is a parameter affecting the shape (outflow height). Through a slight modification, the model can accommodate asymmetrical microbursts with an essentially arbitrary vertical shear profile, the addition of a vortex ring to more closely simulate an actual microburst, and wet microbursts. Given the present state of knowledge concerning wind shear, this model produces geometries that are in excellent agreement with those that have been actually observed. Futhermore, with this more realistic model, we shall be able to simulate radar returns from several different range gates.

4. IMPLEMENTATION

In implementing the actual system, several essential parameters regarding the hardware and data acquisition scheme will have to be determined. These include items such as range and antenna weighting functions, antenna gain, size of the resolution volume scanned by the beam, receiver bandwidth, and pulse repetition time. In this paper we shall only discuss the latter where, ideally, it should be chosen long enough so that returns from consecutive pulses do not overlap and yet short enough so that samples obtained at one range are well correlated for information extraction purposes. We now elaborate.

Since the system studied here will be used in airborne applications, the processing rate, and thus the alert time, is a crucial factor. The processing rate has to be fast enough so that the pilot can be warned well in advance to avoid wind shear. This rate can be improved by overlapping computation time with scanning/sampling time. In this context, the system is thought of as two separate units. The first is a radar that is continuously transmitting and receiving signals and a sampler that is sampling the received signals and storing them in memory banks according to their range as shown in Fig. 3. The second unit is a processor that is computing estimates and making decisions. While the processor is processing returns from the first M pulses, the returns of the second M pulses are being sampled and stored in memory. In order to do this overlapping, the processor must process the data at a rate higher or at least equal to the rate at which

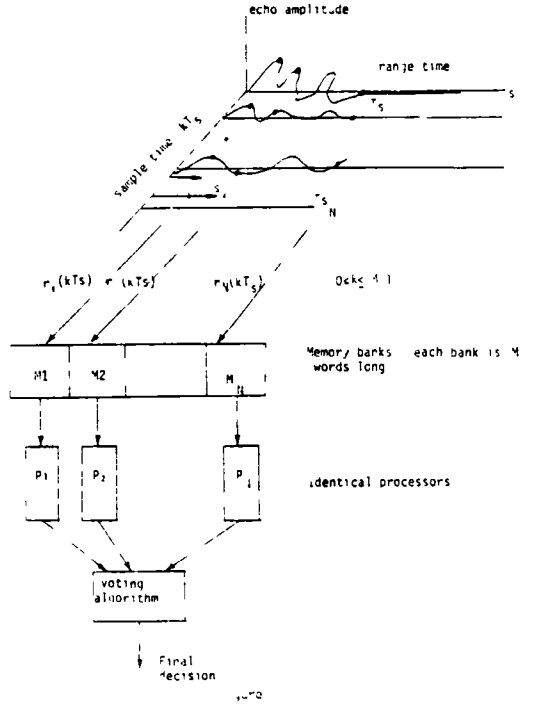

the data are received For example, if M = 256 and T_s = 1ms, then this rate is 1/25 6 kHz. Such a high rate may not (depending on the value of N) be achieved with a serial processor Instead, one can use a number of identical processors that run in a parallel fashion, see Figure 3 Each processor is small, fast, and responsible for all the computation required at one range gate The computation consists of spectral estimation, filtering, and abrupt jump monitoring In addition to achieving a high processing rate, this scheme is advantageous in that N decisions, regarding the presence or absence of wind shear, at N range gates will be made all at once This is a very informative aspect because in a way it reflects the dimension of a microburst along the beam axis and it allows for rejection of false alarms on part of the individual processors, i e., a microburst should trigger the output of more than one processor. Thus, a voting algorithm, based on prespecified criteria, can be implemented to produce one final decision

A large number of range time samples, however, imposes a limitation on our processing scheme. A large N requires a large number of processors which could be impractical due to space and power limitations on board an aircraft. In such a case the N discrete sequences can be divided into groups each of which is J sequences long, where J is a submultiple of N Every group will be processed in a parallel fashion on J processors, while the different groups are fed serially. Even in this mixed processing, an important improvement in the processing rate would be achieved

5 CONCLUSION

The preliminary findings described above strongly suggest that the first-passage analysis we have adopted provides a viable approach to the problem of identifying the onset of wind shear The results to date center on an idealized symmetric geometry for the wind pattern and have neglected noise processes specifically related to ground clutter It is not expected, however, that the relaxation of these constraints will alter the basic conclusion Future work will incorporate real data and thus will be able to determine the ultimate efficacy of the approach

Acknowledgement This work is supported by a grant from the NASA Langley Research Center in Hampton, Virginia

REFERENCES

1 T Fujita, The Downburst, SMRP Research Paper Number 210 The University of Chicago, 1985

2 National Research Council, Report of the Committee on Low-Altitude Wind Shear and its Hazard to Aviation, National Academy Press, Washington, D C 1983

3 R Doviak and J Zrnic, Doppler Radar and Weather Observations, Academic Press 1984

4 M H A Davis, The Application of Nonlinear Filtering to Fault Detection in Linear Systems, IEEE Trans on Automatic Control, April 1975 pp 257-259

5 H Van Trees, Detection, Estimation, and Modulation Theory, vol III, Wiley, 1971

6 A Jazwinski, Stochastic Processes and Filtering Theory, Academic Press, 1970.

7 G Franklin and J Powell, Digital Control of Dynamic Systems, Addison-Wesley, 1980

APPENDIX B

Simulated results of state estimates

Representative state estimates utilizing the model in (4') and (5') and the filter in (10') and (11') (with SOT = 0) are shown below for one range gate. The filter is implemented in terms of a square-root algorithm; the computer program that produced these results on a CDC Cyber 180 computer is also given.

The values of the parameters used in the simulation are as follows:

$A = 1.0$ $\quad F = 10^{-4}$ $\quad P_{11} = 1.0,\ P_{22} = 1.0$

$V_c = 1.0$ $\quad G = 10^{-4}$ $\quad P_{33} = 20.0$

$W_c = 0.5$ $\quad H = 10^{-4}$ $\quad P_{44} = 0.5$

$B_c = 0.5$ $\quad K_1 = 32\ (\equiv M)$ $\quad P_{ij} = 0.1,\ i \neq j$

$U_c = 10^{-5}$ $\quad x_0 = 10.0,\ \hat{x}_0 = 10.0$

$\lambda = 0.1$ $\quad b_0 = 40.0,\ \hat{b}_0 = 30.0$

$\nu = 0.15m$ $\quad \psi_0 = 1.0,\ \hat{\psi}_0 = 0$

In each of the four graphs that follow, the true value of the state is denoted with a solid line and its estimate is denoted with a dotted line. For example, for state x, the wind velocity before wind shear, the true value is Sx and its estimate is Fx; for state z, the true and estimated

values are Sz and Fz, respectively; etc. Also, each graph shows 63 time samples, with the jump time (indicating the onset of wind shear) occurring at time increment 32.

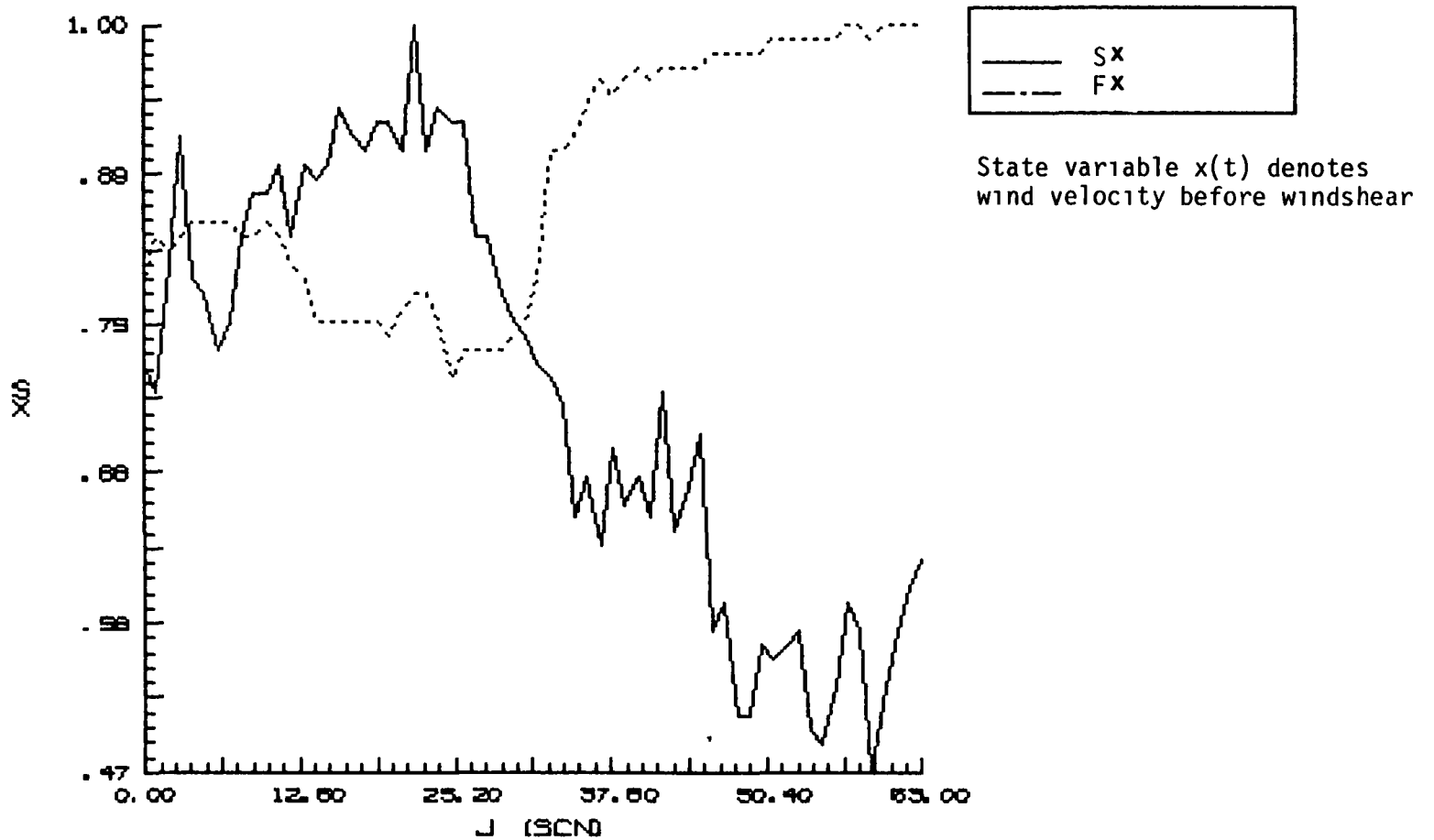
1.00
.89
.79
.68
.58
.47
XS
0.00
12.60
25.20
37.80
50.40
63.00
J (SCN)
SX
FX
State variable x(t) denotes
wind velocity before windshear

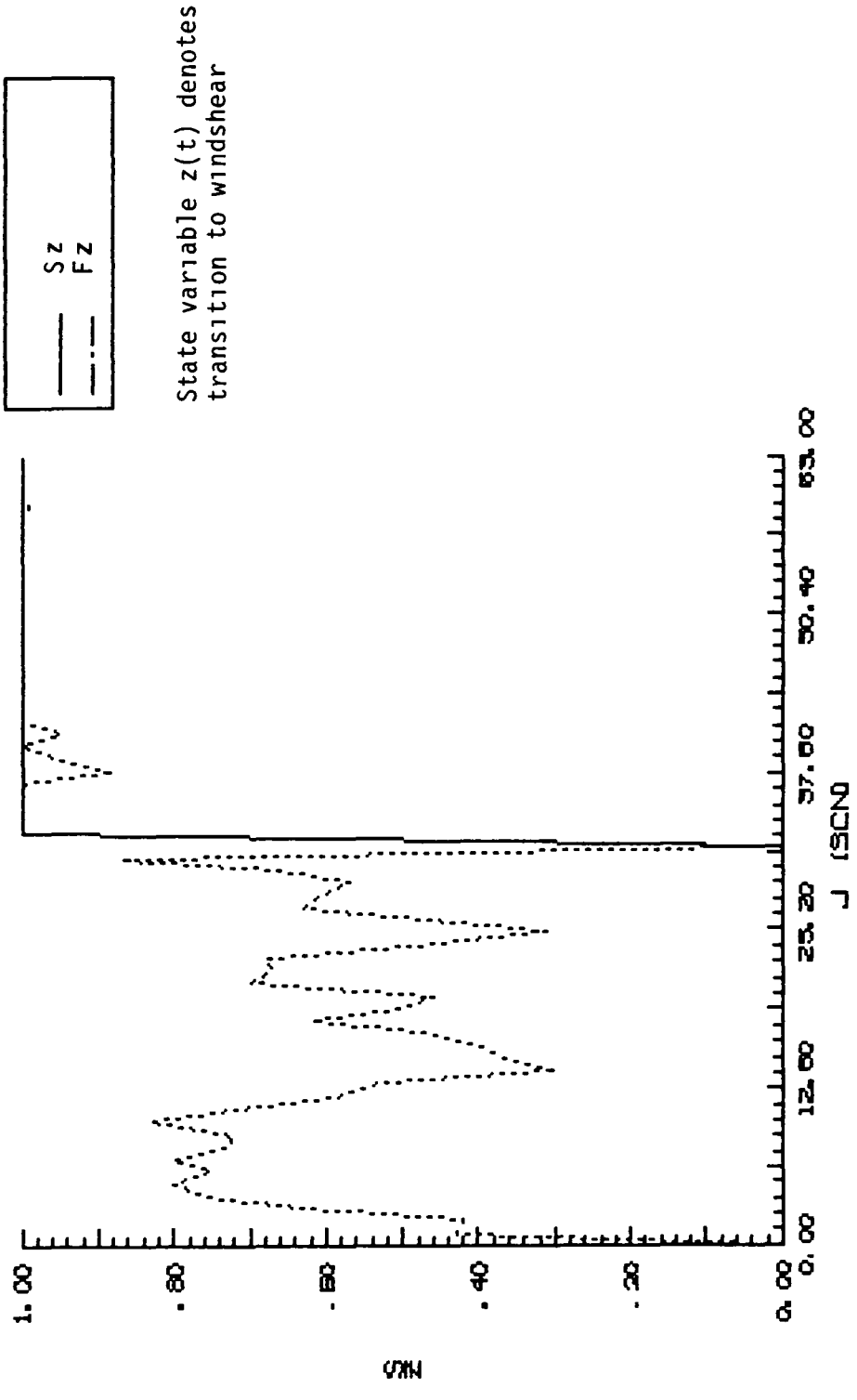
Sz
Fz
State variable z(t) denotes
transition to windshear
1.00
.80
.60
.40
.20
0.00
0.00
12.60
25.20
37.80
50.40
63.00
J (SCN)

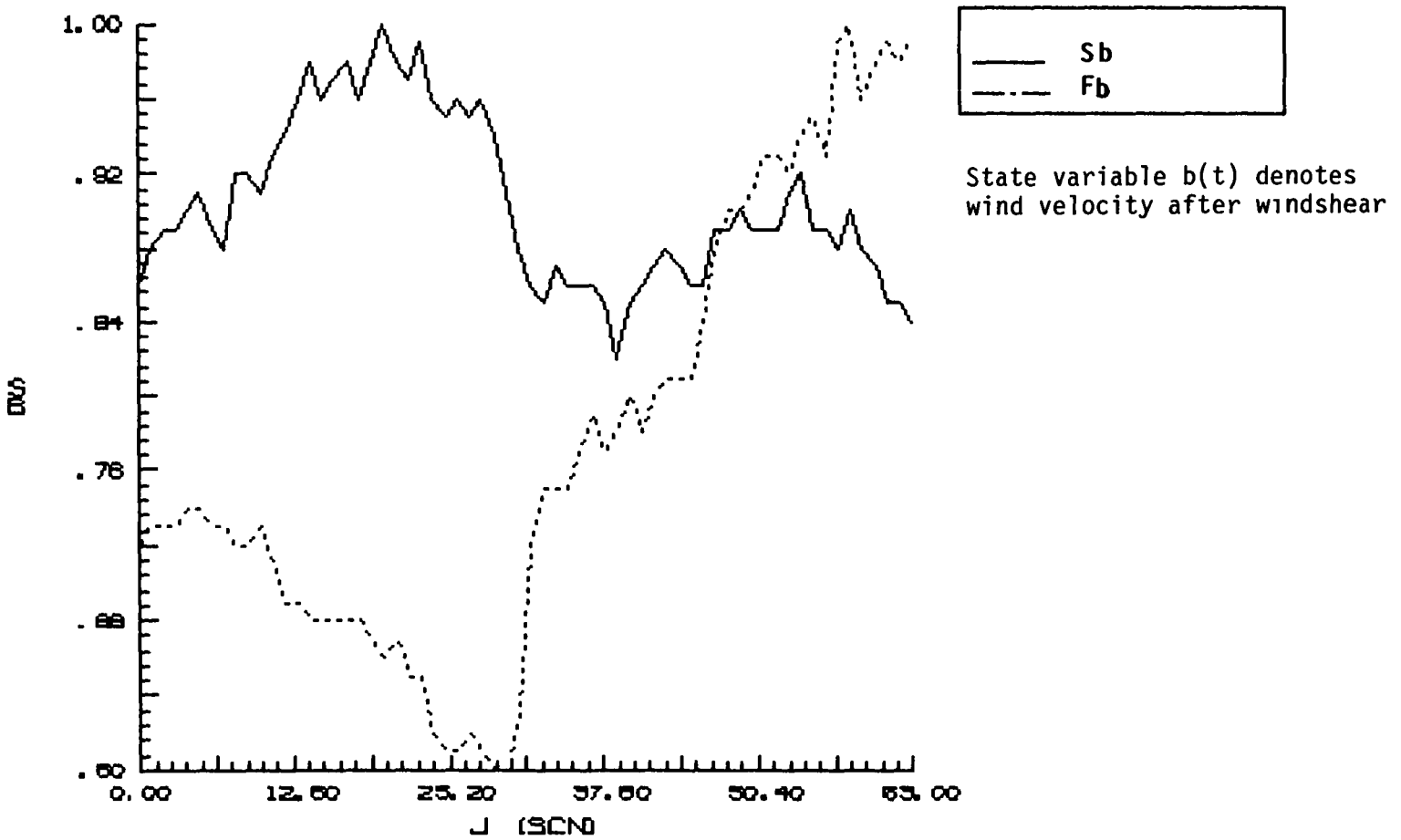
1.00
.92
.84
.76
.68
.60
0.00
12.60
25.20
37.80
50.40
63.00
J (SCN)
Sb
Fb
State variable b(t) denotes
wind velocity after windshear

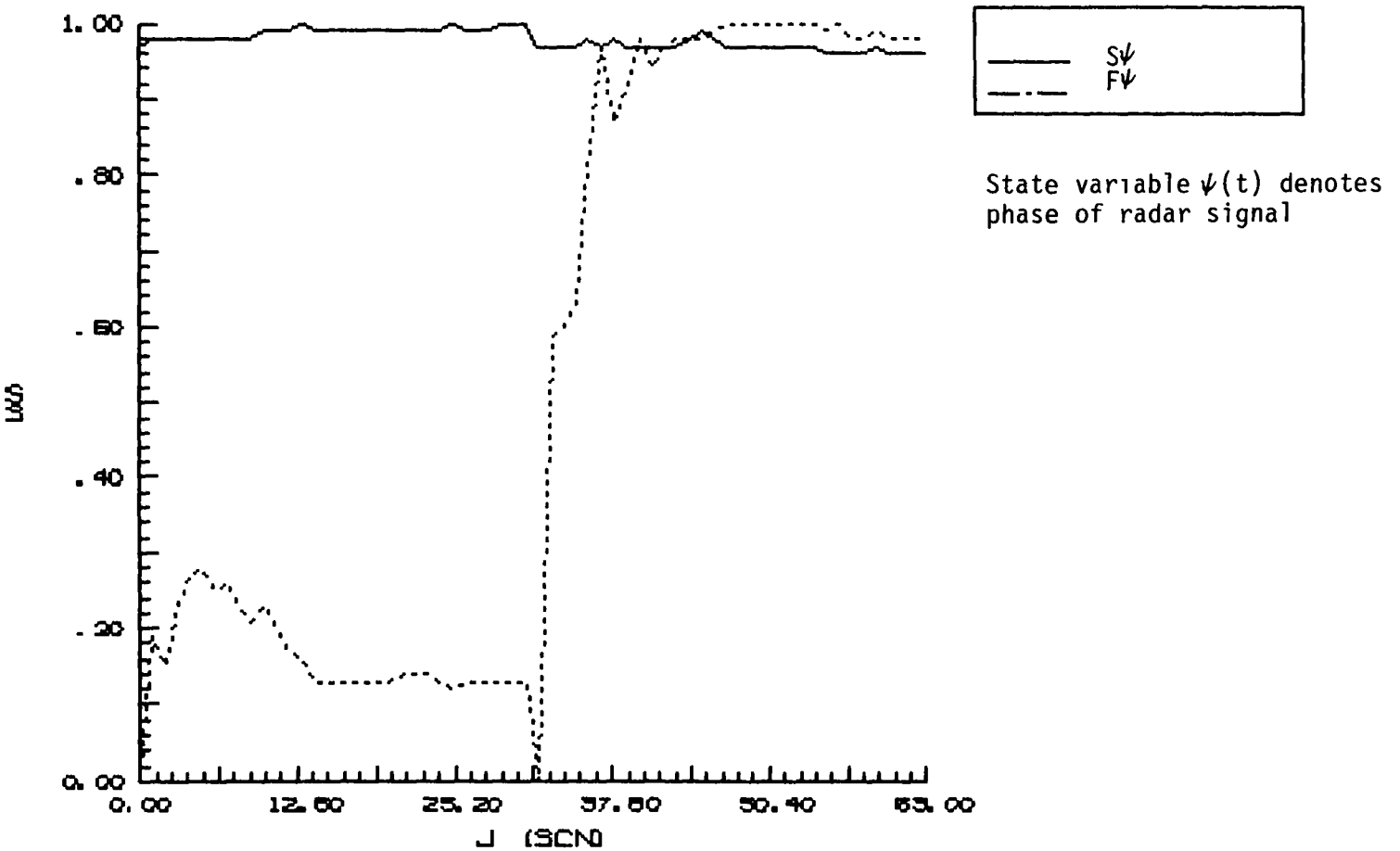
1.00
.80
.60
.40
.20
0.00
0.00
12.60
25.20
37.80
50.40
63.00
J (SCN)
SΨ
FΨ
State variable $\Psi(t)$ denotes phase of radar signal

```
      PROGRAM OPEXEC(INPUT,OUTPUT,TAPE10=INPUT,TAPE20=OUTPUT)
C
C
C
      INTEGER K,K1,I,J,I1,J1
      REAL    SX(0:127),SZ(0:127),FX(0:127),FZ(0:127),FB(0:127),
     1        DF(0:127),P11(0:127),P12(0:127),P13(0:127),P22(0:127),
     2        P23(0:127),P33(0:127),SB(0:127),FS(0:127),P14(0:127),
     3        P24(0:127),P34(0:127),P44(0:127),SS(0:127),
     4        U(4,4),V(4,8),D(4),T(8),W(4),N(4),
     5        WC,VC,AC,CK,FK,WL,ER,WK,VK,FE,CF,SA,FA,F,G,BK,EC,
     6        C0,C4,C6,A1,A2,A3,A4,A5,A6,SI,TMP,AL,USX,USB,UFX,UFB,
     7        B7,BB,UK,UC,H,C7,S1,S2,S3,S4,S5,D2,D3,D4,WI,ER1
      DATA    SX(0),FX(0),SB(0),FB(0),SZ(0),FZ(0),DF(0),FS(0),WL,CF,
     1        P12(0),P13(0),P23(0),P14(0),P24(0),P34(0),SS(0)/2*10.0,
     2        40.0,30.0,4*0.0,1500.0,0.0,6*1.0,1.0/
C
C
C
C MAIN PROGRAM
C
      READ(10,10)K1
10    FORMAT(I2)
      WRITE(20,15)
15    FORMAT(5X)
      READ(10,20)VC,WC,BC,UC,A,F,G,H,ER,P11(0),P22(0),P33(0),P44(0)
20    FORMAT(F7.4)
      WRITE(20,40)WC,VC,BC,A,F,G,K1
40    FORMAT('WC=',F5.2,2X,'VC=',F5.2,2X,'BC=',F6.3,2X,'A=',F5.2,
     1       2X,'F=',F5.4,2X,'G=',F5.4,2X,'K1=',I2///)
      S=.5
      CALL PARSET(S)
      WRITE (20,100)
100   FORMAT('  W',5X,'FX',4X,'FZ',6X,'SB',6X,'FB',6X,'FS',6X,
     1       'P11',5X,'P22',5X,'P33',5X,'P44')
C
      UFX=10.0*F
      USX=UFX
      UFB=30.0*G
      USB=40.0*C
      F=F-1.0
      G=G-1.0
      H=H-1.0
      ER1=ER
      ER=ER-1.0
      A=SQRT(2.0*A)
      CC=2.0*3.14159**2
      FE=2.0*CC/WL
      CF=CF*CC
C
      DO 1000 I=0,3
      DO 500 K=0,31
      IF (K .NE. 0) GOTO 102
      D(4)=P44(0)
      U(3,4)=P34(0)/D(4)
      D(3)=P33(0)-D(4)*U(3,4)**2.0
      U(2,4)=P24(0)/D(4)
      U(2,3)=(P23(0)-U(2,4)*U(3,4)*D(4))/D(3)
      D(2)=P22(0)-D(3)*U(2,3)**2.0-D(4)*U(2,4)**2.0
      U(1,4)=P14(0)/D(4)
      U(1,3)=(P13(0)-U(1,4)*U(3,4)*D(4))/D(3)
      U(1,2)=(P12(0)-U(1,3)*U(2,3)*D(3)-U(1,4)*U(2,4)*D(4))/D(2)
      D(1)=P11(0)-D(2)*U(1,2)**2.0-D(3)*U(1,3)**2.0-D(4)*U(1,4)**2.0
      T(5)=0
```

```
      T(6)=FB1
      T(7)=FC
      T(8)=UC
      U(1,1)=1.C
      U(2,2)=1.C
      U(3,3)=1.C
      U(4,4)=1.0
C
102   J=K+I*32
      D2=1.C+FZ(K)*ER
      D3=-FB(K)*G+FX(K)*F
      D4=-FB*FZ(K)
      FA=FE*REAL(K+1)*(FB(K)*FZ(K)*G*ER-D2*FX(K)*F)
      CK=COS(CF*REAL(K+1)+FA-FS(K)*H)
      HK=A*SIN(CF*REAL(K+1)+FA-FS(K)*H)
      C4=FC*REAL(K+1)*AX*CK
      CF=A*CK
      R1=RANF()
      R2=RANF()
      R3=RANF()
      R4=RANF()
      R5=RANF()
      R6=RANF()
      R7=RANF()
      R8=RANF()
      WK=SQRT(-2.0*WC*ALOG(R1))*COS(CC*R2)
      VK=SQRT(-2.C*VC*ALOG(R3))*COS(CC*R4)
      BK=SQRT(-2.C*BC*ALOG(R5))*COS(CC*R6)
      UK=SQRT(-2.C*UC*ALOG(R7))*COS(CC*R8)
C
      SZ(K+1)=0.0
      IF (J+1 .GT. K1) THEN
        SZ(K+1)=1.0
      ENDIF
      SY(K+1)=-SY(K)*F+WK+USX
      SB(K+1)=-SB(K)*C+BK+USB
      SS(K+1)=-SS(K)*H+UK
      SA=FE*REAL(K+1)*(SB(K+1)*SZ(K+1)+(1.0-SZ(K+1))*SX(K+1))
      OF(K+1)=A*SIN(CF*REAL(K+1)+SA+SS(K+1))+VK
C
      S1=CR(K+1)-HK
      S2=((P11(K)*F**2.C+WC)*D2+ER*F*P12(K)*D3+G*F*P13(K)*D4)*C4
     1    +H*F*P14(K)*C6
      S3=(ER*F*P12(K)*D2+(ER1*(1.0-FZ(K))+P22(K)*ER**2.0)*D3+ER*
     1    G*P23(K)*D4)*C4+ER*H*P24(K)*C6
      S4=(G*F*P13(K)*D2+ER*G*P23(K)*D3+(P33(K)*G**2.C+BC)*D4)*C4
     1    +H*G*P34(K)*C6
      S5=(H*F*P14(K)*D2+ER*H*P24(K)*D3+H*G*P34(K)*D4)*C4+
     1    (P44(K)*H**2.0+UC)*C6
      WI=C4*(D2*S2+D3*S3+D4*S4)+C6*S5+VC
C
      FY(K+1)=-FY(K)*F+S2/WI*S1+UFX
      FZ(K+1)=-ER*FZ(K)+S3/WI*S1+ER1
      FB(K+1)=-FB(K)*G+S4/WI*S1+UFB
      FS(K+1)=-FS(K)*H+S5/WI*S1
C
      DO 110 J1=1,3
      DO 105 I1=1,4
        V(I1,J1)=C.C
105   CONTINUE
110   CONTINUE
      DO 115 I1=1,4
        T(I1)=C(I1)
115   CONTINUE
```

```
      T(6)=ER1*(1.0-FZ(K))
      W(1,5)=1.0
      W(2,6)=1.0
      W(3,7)=1.0
      W(4,8)=1.0
      W(1,1)=-F
      W(1,2)=-F*U(1,2)
      W(1,3)=-F*U(1,3)
      W(1,4)=-F*U(1,4)
      W(2,2)=-ER
      W(2,3)=-ER*U(2,3)
      W(2,4)=-ER*U(2,4)
      W(3,3)=-G
      W(3,4)=-G*U(3,4)
      W(4,4)=-H
C
      DO 145 J1=4,1,-1
      TMP=0.0
      DO 120 L=1,8
        TMP=TMP+W(J1,L)**2.0*T(L)
120   CONTINUE
      D(J1)=TMP
      DO 130 I1=1,J1-1
        TMP=0.0
        DO 125 L=1,8
        TMP=TMP+W(I1,L)*W(J1,L)*T(L)
125     CONTINUE
        U(I1,J1)=TMP/D(J1)
130   CONTINUE
      DO 140 I1=1,J1-1
        DO 135 L=1,8
        W(I1,L)=W(I1,L)-U(I1,J1)*W(J1,L)
135     CONTINUE
140   CONTINUE
145   CONTINUE
C
      V(1)=C4*D2
      V(2)=C4*(U(1,2)*D2+D3)
      V(3)=C4*(U(1,3)*D2+U(2,3)*D3+D4)
      V(4)=C4*(U(1,4)*D2+U(2,4)*D3+U(3,4)*D4)+C6
      DO 150 I1=1,4
        W(I1)=D(I1)*V(I1)
150   CONTINUE
C
      AL=VC+W(1)*V(1)
      D(1)=D(1)*VC/AL
      T(1)=W(1)
      T(2)=0.0
      T(3)=0.0
      T(4)=0.0
      DO 170 J1=2,4
        TMP=AL
        AL=AL+W(J1)*V(J1)
        D(J1)=D(J1)*TMP/AL
        DO 155 I1=1,4
          W(I1,1)=U(I1,J1)
155     CONTINUE
        DO 160 I1=1,4
          U(I1,J1)=U(I1,J1)-V(J1)*T(I1)/TMP
160     CONTINUE
        DO 165 I1=1,4
          T(I1)=T(I1)+W(J1)*W(I1,1)
165     CONTINUE
170   CONTINUE
```

```
C
      P11(K+1)=D(1)+D(2)*U(1,2)**2.0+D(3)*U(1,3)**2.0+D(4)*U(1,4)**2.0
      P12(K+1)=D(2)*U(1,2)+D(3)*U(1,3)*U(2,3)+D(4)*U(1,4)*U(2,4)
      P13(K+1)=D(3)*U(1,3)+D(4)*U(1,4)*U(3,4)
      P14(K+1)=D(4)*U(1,4)
      P22(K+1)=D(2)+D(3)*U(2,3)**2.0+D(4)*U(2,4)**2.0+D(2)
      P23(K+1)=D(3)*U(2,3)+D(4)*U(2,4)*U(3,4)
      P24(K+1)=D(4)*U(2,4)
      P33(K+1)=D(3)+D(4)*U(3,4)**2.0
      P34(K+1)=D(4)*U(3,4)
      P44(K+1)=D(4)
C
      IF (FZ(K+1) .GT. 1.0) THEN
         FZ(K+1)=1.0
      ENDIF
      IF (FZ(K+1) .LT. 0.0) THEN
        FZ(K+1)=0.0
      ENDIF
      IF (P22(K+1) .LT. .001) THEN
        P22(K+1)=.001
      ENDIF
C
C
100   WRITE(20,200)K,FX(K),FZ(K),SP(K),F3(K),FS(K),
     1                P11(K),P22(K),P33(K),P44(K)
200   FORMAT(I3,9F8.2)
C
500   CONTINUE
C
      WRITE (20,600)
600   FORMAT(5X)
1000  CONTINUE
      STOP
      END

14.13.49 UCLP, AA, TPRNT01,       0.295KLNS.        ** END OF LISTING **
```

End of Document